EVALUATION OF OPTICAL ABSOLUTE NAVIGATION METHOD USING CRATERS FOR LUNAR SOUTH POLE LANDING

Dr. Svenja Woicke[(1)] and Hans Krüger[(2)]

[(1)]German Aeropsace Centre, Robert-Hooke-Straße 7, 28359 Bremen, Germany, +49 421 244420-1871, svenja.woicke@dlr.de
[(2)]German Aeropsace Centre, Robert-Hooke-Straße 7, 28359 Bremen, Germany, +49 421 24420 1126, Hans.Krueger@dlr.de

ABSTRACT

The Moon is an ever trending target for many current and future missions. Also ESA wants to land on the Moon within the context of the European Large Logistics Lander program. Likewise many of the other missions ESA is specifically interested to land very close to the Lunar south pole. While the pole is a very interesting scientific target it is very demanding from a technical point of view. The terrain is rough and the illumination conditions are extremely challenging. Precision landing capabilities are required, calling for the use of absolute navigation. In this paper it is demonstrated that vision based absolute navigation can be used even in these challenging illumination conditions. In the paper it is shown that the south pole is sufficiently illuminated to design approach trajectories viable for optical navigation in a robust manner. Furthermore, we demonstrate on one such trajectory that absolute navigation can deliver results up to at least 600 m above the south polar landing site. Concluding that DLR's crater navigation system is a key asset for safe and successful landing on the Moon also at the lunar south pole.

1 INTRODUCTION

All mayor space agencies and many private enterprises aim to land at the Moon in the upcoming years. Also ESA desires to land on the Moon within the European Large Logistics Lander (EL3) program. EL3 will consist of multiple landers, each aiming for a different landing site, with the launch of the first lander planned for the end of this decade. To this end, the program requires a GNC system that can reach any desired landing site on the entire Moon. It therefore needs to be highly flexible requiring only little adaptations for each specific landing site. Likewise almost all future landing missions, EL3 requires precision landing capabilities to deliver the lander and payloads with high accuracy, enabling landing in hazardous terrain and very close to surface assets from previous missions. To land with such a high accuracy it is a pre-requisite to include an absolute navigation method into the GNC system, which makes the lander Moon-centered Moon-fixed (MCMF) pose observable. To date this is still a rather novel technology, which has been employed for the Perseverance lander on Mars[1] and for the Chang'e Program by the Chinese Space Agency only, where no conclusive information on the absolute navigation system has been published. It must thus nevertheless still be considered a novel technology.
Absolute navigation always requires to determine the lander's pose and orientation with the aid of some reference which is known in an absolute reference frame. On the Moon this is

most commonly done using surface features derived from the great amount of observation data available from prior lunar missions such at the Lunar Reconnaissance Orbiter (LRO) and Kaguya. Multiple different approaches exist, both based on active (Lidar,Radar) and passive sensors (cameras). Camera based methods usually rely either natural features, such as craters, or more 'artificial' features, described by so-called feature descriptors. Radar and Lidar based techniques usually perform some form of template matching based on DEM data, for example using terrain lines. In this paper an optical method using craters as absolute features is used. Craters are an excellent choice of feature since they can be represented such to be invariant to scale and rotation, while the required databases are not to heavy in terms of storage requirements.
This paper will first introduce DLR's crater navigation system CNav. After this a closer look is given to the Lunar south pole and the challenges it poses for landing. After this the performance of CNav on the lunar south pole is demonstrated and discussed. The paper closes with conclusions.

2 CNAV

DLR's crater navigation system (CNav), is an absolute navigation system making use of on-board images in conjunction with an on-board crater catalog to determine matches between observed craters and craters present in the catalog. To extract the craters a crater detector is used which extracts craters based on their characteristic pattern of shaded and non-shaded regions. The detector determines the illumination direction internally and does therefore not require any information on the Sun's position as an input. More details about the crater detector can be found in [2], [3]. The crater detector can operate from very low sun elevation up to sun elevations of 50°. At even higher elevations shadowing is greatly reduced and will thus not allow for the successful application of our detection method.
After craters are detected, the detected craters are passed to the matcher. The matcher tries to match the craters against on-board catalogs. For increased robustness and performance the matcher is split into two different matching modes, a acquisition mode, which can be used in the absence of sufficiently accurate state estimates, for example at the beginning of the descent and landing navigation. Since this matcher needs to be highly robust and cannot rely on any form of initial guess, it is slower and has a lower success rate. Once the navigation solution starts to converged based on the solutions obtained in acquisition mode, an sufficiently accurate initial guess can be provided to CNav to enable tracking mode, tracking mode is faster and has a higher success rate than acquisition mode, however it less robust to large inaccuracies in the navigation estimate. Please see [4] for a detailed study of the robustness of both matching methods. CNav chooses the appropriate matching method autonomously and does not require any user input. However, the desired method can be manually be commanded if needed. CNav features an internal match verification stage to ensure that only valid solutions are passed to the navigation system.
CNav operation will likely be stared with one or a couple of solutions obtained via acquisition mode, allowing for the state knowledge to converge, and will then be followed by solutions obtained via tracking mode. Should phases of no-solution occur, for example due to the absence of detectable craters, e.g. in extremely hilly terrain, due to permanently shaded terrain or because the CNav camera temporally did not point to the surface, either tracking mode can re-acquire a solution or acquisition mode will step in should the solution have diverged too much for a successful tracking mode match.
CNav is capable of running at 0.2 Hz in acquisition mode and 1 Hz in tracking mode when

running on high performance spaceflight computing hardware (currently tested on arm-53 and arm-72 based architectures).

2.1 Crater Catalog

Next to the algorithm itself one the key assets for CNav is the crater catalog, a global catalog needs to be available to provide global access to the Moon. DLR has created its own global crater catalog containing more than 40 Million craters. The crater data has been determined applying an in-house processing flow, using geo-referenced visual and 3D map data. Two methods are currently used for finding lunar craters in publicly available data. The first method applies the CNav detector stage directly to Kaguya morning maps [5], resulting in a very large set of crater candidates. Each one has several parameters attached such as the crater center's longitude and latitude, and its radius. All crater candidates are then looked up in the Kaguya-LRO-merged map [6] to complement the parameter with the altitude over lunar radius. Simultaneously the candidates are checked for certain geometric metrics to remove false craters. This first method covers the lunar surface in the latitude range of 60° to −60°. A second method uses the LRO LOLA based DEMs to render images of the lunar in illumination conditions favorable for the CNav detector. The set of resulting candidates is then further processed using the LOLA DEMs for altitude look-up. The south pole part of our global catalog is based on [7]. It contains 712481 craters. Please see figure 1 for a visualization.
In addition to this global catalog it is possible to extract more craters from higher resolution DEMs and add these to the catalog locally. However, these craters are only of interest for the parts of the landing where the lander is already very low. Therefore at the moment, we only extract and add these craters on a per-mission basis.
From the global catalog, missionized crater catalogs are constructed, as the full crater catalog is too large for on-board storage but will also propose performance challenges when trying to match against such a large database. It is a future goal to extend CNav with a on-board algorithm which can extract only necessary craters from the global catalog and thereby increase robustness for back up maneuvers, open up new applications, such as continuous estimates on an orbiter and will decrease the missionisation effort.

3 THE SOUTH POLE

The intention of this work is showing that CNav is successfully operating under the most demanding conditions on the Moon. Given sufficient performance there, will let us consider CNav to be in principle qualified for offering global access to landing missions. CNav requires illuminated terrain and the abundance of craters. These conditions, in particular the one with regard to illumination, are hardest to meet in the polar regions. This is mainly due to its persistent low Sun elevation and permanently shadowed regions. For this reason we chose the south pole as a landing site of a demo mission. In principal, of course, the north pole offers very similar conditions. However, due to the high interest directed towards the south pole this region is studied here.
The Moon's inclination is approximately 1.54° relative to the ecliptic. Moreover, its shape, which significantly deviates from a perfect sphere, leads to regional variations in illumination and shadowing contrary to what would be expected if it was spherical. This results in unique lighting conditions near the Moon's south pole. These conditions include half-year cycles of day and night, periodic areas of constant shadow, and the Sun persistently appearing at a low angle. As depicted in figure 3, from the south pole to about −85° latitude, the lunar surface varies in

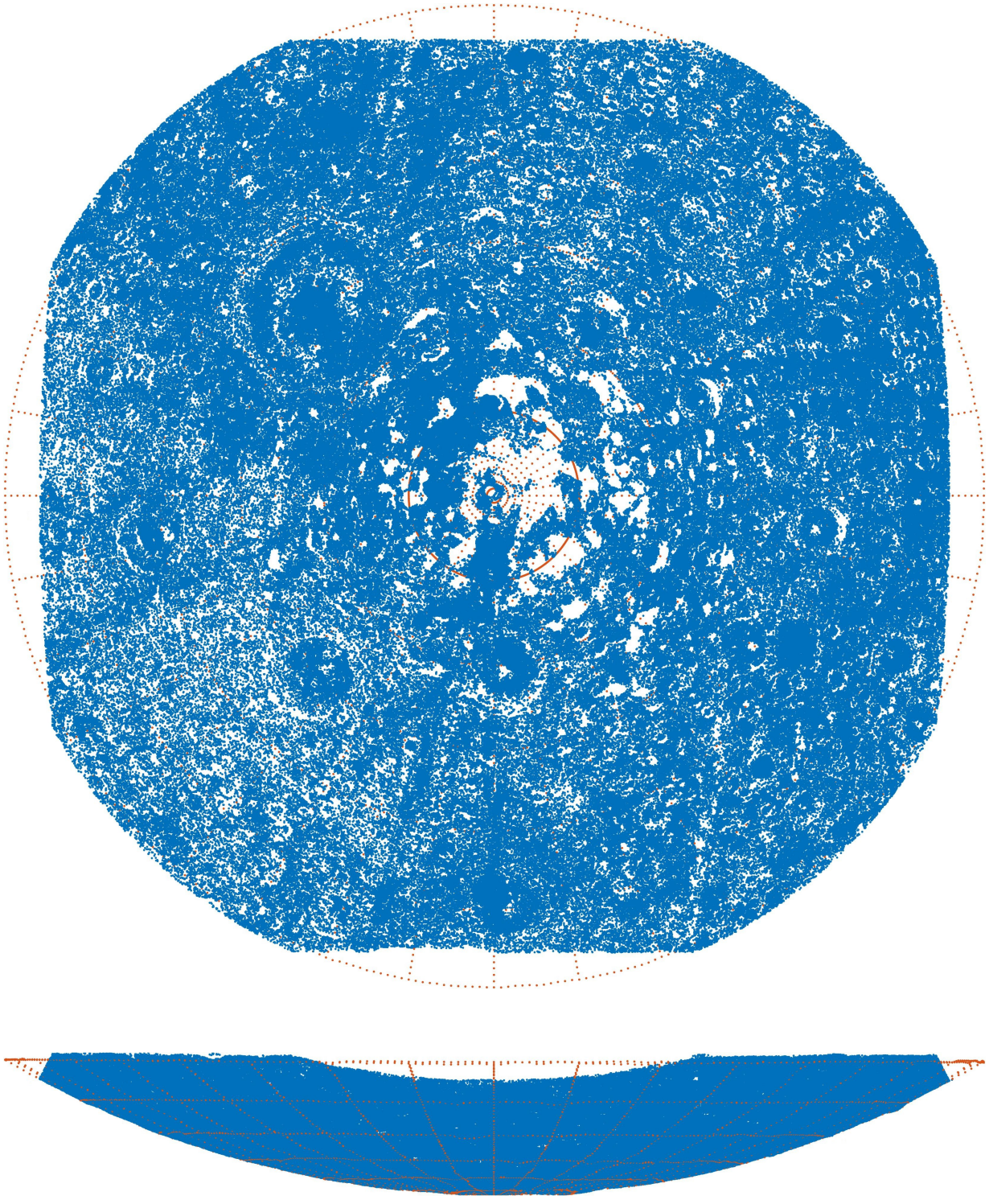

Figure 1: South pole part of the global catalog containing 712481 craters. Each crater is displayed as point. The map covers latitudes from $-60°$ to $-90°$.

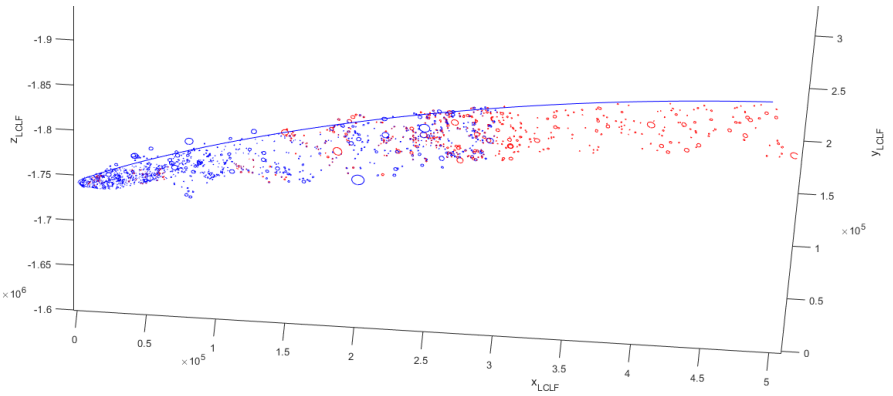

Figure 2: Crater catalog below polar descent trajectory, locally added craters indicated in blue, global catalog in red.

elevation by roughly −5.5 km to 7 km, relative to the Moon's radius of 1737.4 km. This causes some regions to be lit when the Sun is below the horizon and other areas to remain in shadow due to higher terrain blocking the sunlight, even when the Sun is above the horizon. Some elevated features like ridges or crater rims can enjoy near-continuous sunlight during a south pole winter [8]. On the positive side in terms of lighting, geometric features such as inclined planes exist. Due to their slope, some of these planes are illuminated at local Sun elevations higher than 1.54°.

Consequently, it seems a plausible assumption that there should be paths that provide a terrain sufficiently lit for CNav to satisfactory function. Choosing an actual trajectory guiding the lander to the south pole, involves an iterative process. It includes visual inspection using a rendered birds-eye view and navigation camera images, cataloging craters for the mission, operating CNav in an open-loop mode, and readjusting the trajectory geometry as per mission objectives. The last three steps in particular are labor-intensive.

In order to narrow down the space of trajectories before commencing open-loop testing, the local Sun elevation at Shackleton crater was assessed using SPICE [9]. As a second metric it was analyzed to what grade the vicinity of the south pole is illuminated by the Sun. This information is obtained by simulating a camera, which is placed at a certain altitude over the landing site with a nadir viewing direction. Then, one image is rendered per day over the course of the observation period from 01.12.2024 to 30.11.2024. For each image the number of dark pixels, characterized by an intensity of 0, is counted and related to the remaining number of pixels. An observation camera with a FOV of 80° and an altitude of 100 km was selected. The observed area covers distances between 120 km and about 150 km from the landing site. Please refer to figure 6 for reference. There, the biggest yellow circle marks −86° latitude. In the corner parts of the image parts of the area until approximately −85° latitude can be seen. One degree on the lunar circumference covers 30.3 km. At latitudes higher than −85° the Sun is already significantly higher above the horizon, therefore analysis of metric 2 was restricted to the region of interest discussed here.

The results of metric one, the Sun elevation, are shown in figure 5. The Sun's elevation at Shackleton changes over a one-year period, reaching its peak once annually, observed twice, once in mid-December 2024 and again at the end of November 2025. It seems logical for this study to target a landing date when the local Sun elevation is at its highest. To further refine the selection, it was assumed that the Earth must be visible from the trajectory, thereby eliminating about half of all potential polar trajectory approaches. Due to constraints in the

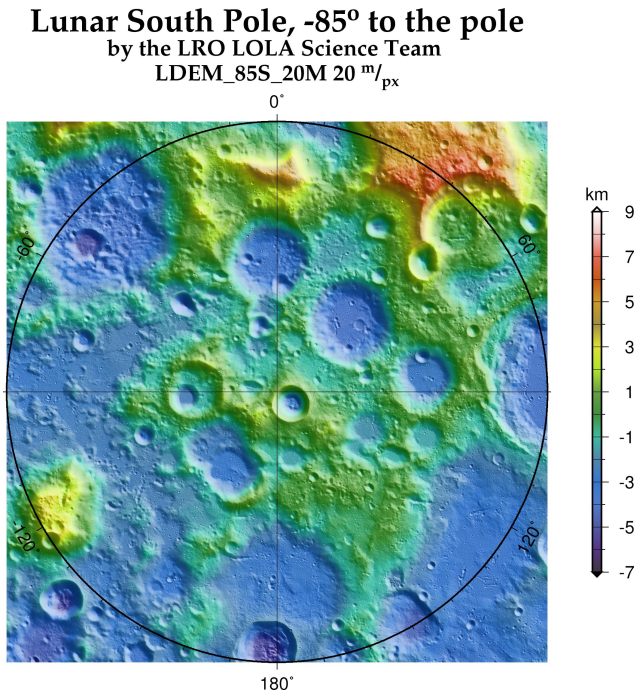

Figure 3: Variability of terrain in the lunar south pole region in a range of −5.5 km to 7 km [10].

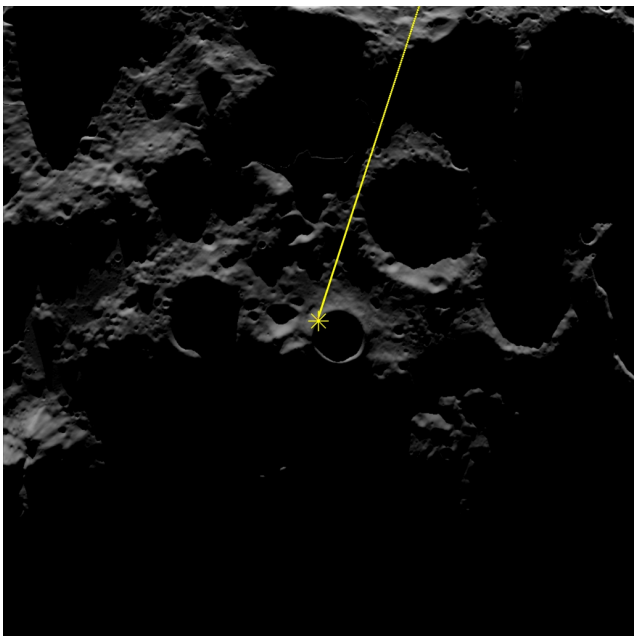

Figure 4: Bird's eye view rendering for 16.12.2024. Yellow line: Final part of candidate trajectory. Yellow star: landing site at Shackleton rim.

study an earlier date was preferred, and thus the month of December around the mid December peak was selected for further study. A set of 31 bird's eye view images were rendered (two of them shown in 6), one for each day in December 2024, revealing two promising approach directions. One of these will be discussed in greater detail in this paper. The latter part of the selected trajectory is displayed in figure 4.
The results of metric two, the share of illuminated surface in the landing region, shows a monthly variation as well as a slower variability over the year. In the study two days in December have been found suitable for CNav. One of them is on 16th of December, which is situated at the monthly minimum of 19% of illuminated pixels. Here, we conclude that more research is required to draw conclusions on how to use this metric for pre-selecting suitable landing dates.

4 CNAV PERFORMANCE FOR SOUTH POLE LANDING

As we have discussed before the south pole is a challenging landing site, however in the previous chapter we have demonstrated that landing at the south pole should be possible even with optical methods. To demonstrate that CNav can be applied for landing at or close to the south pole, we selected a trajectory towards the real south pole, as in terms of crater detection and matching this will pose the most challenging conditions. Realistically speaking any selected landing site will always be slightly off the real south pole. Since the purpose of this work is to demonstrate CNav's performance on any landing in the south pole region the focus was on selecting the most challenging trajectory not the most realistic one in terms of a full mission.
We have rendered the images using DLR's in-house rendering tool SensorDTM[11] at 1 Hz steps. The analysis focuses on the final part of the descent, as for the crater navigation the performance at low altitudes in combination with the challenging polar illumination conditions are the aspects under study. CNav's performance at higher altitudes and non-polar landing sites has already been demonstrated in our earlier work[4]. The camera has a nadir viewing directions during the horizontal phases of the descent, which means that after pitch over the

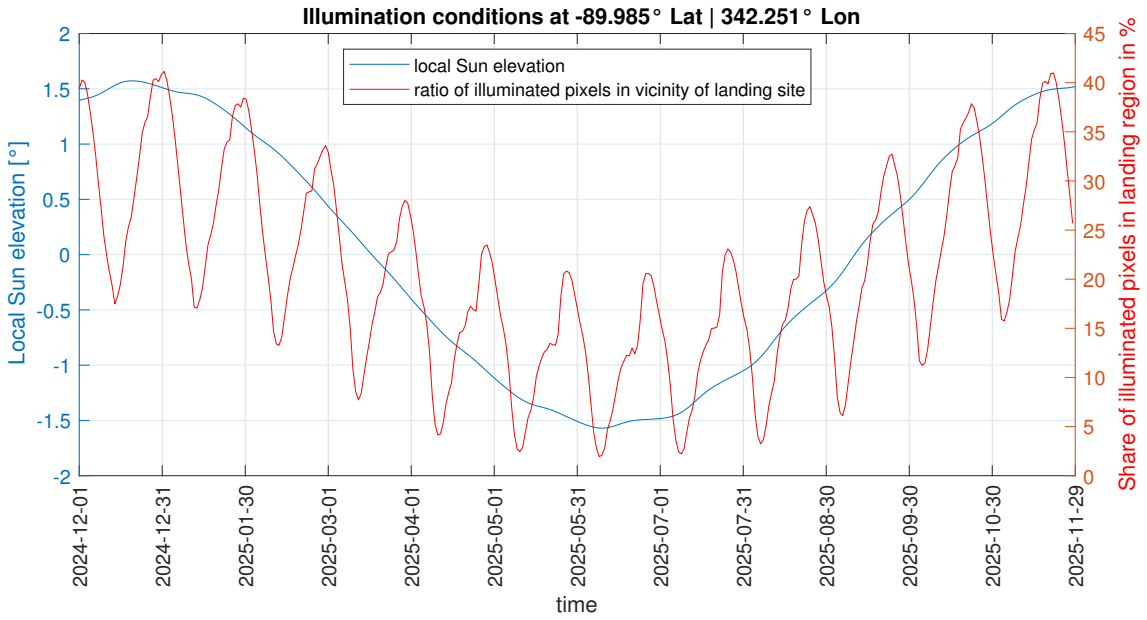

Figure 5: Sun elevation on Shackleton crater rim from December 2024 to November 2025.

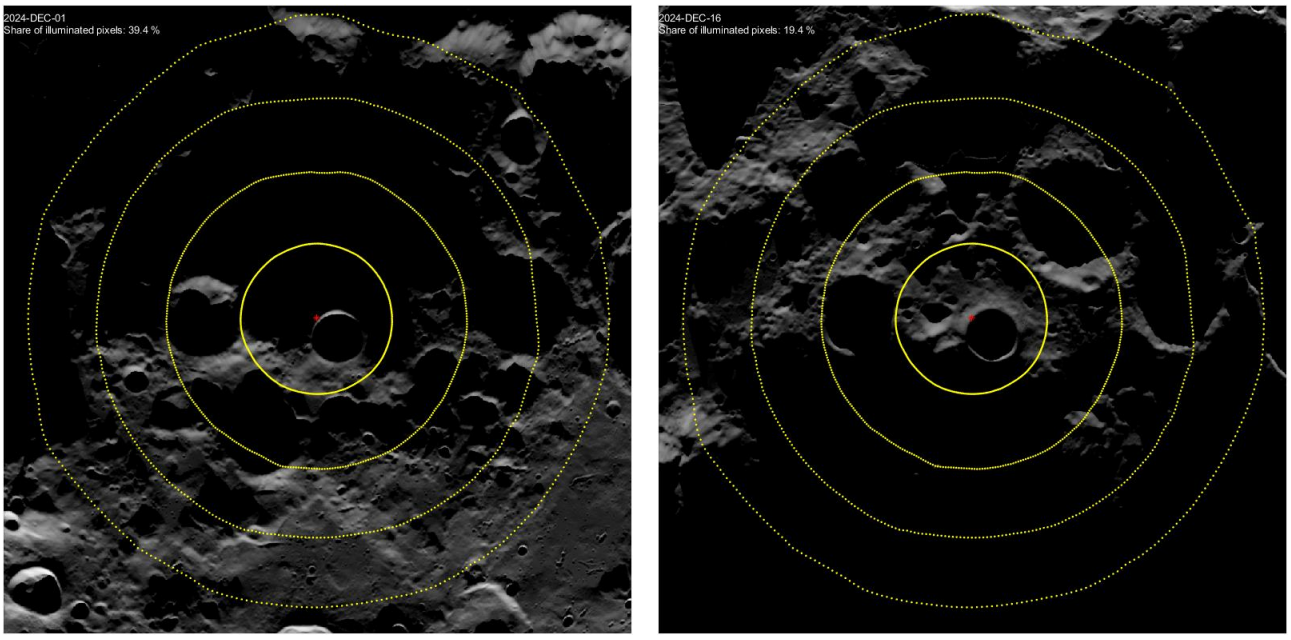

Figure 6: Renderings show illumination conditions on two days in the first two weeks in December 2024. The landing site at Shackleton is marked with a red star. The yellow circles mark latitudes 1° apart. The inner yellow circle marks a latitude of -89°.

camera looks to the surface under a very shallow angle. Note, that this is not the only possible set-up, a more forward looking viewing direct during the first part and thus a close to vertical viewing direction after pitch over could also be considered. Over all the system is very flexible to camera mounting and can also operate when the horizon is in the image and/or parts of the spacecraft are visible in the image.
In order to demonstrate CNav's capabilities at the south pole independent of a full GNC simulation, we have used a set up where CNav is the only source of measurement. In the past we have used CNav purely open-loop to investigates its abilities on any given trajectory, meaning that we have used a pose derived from the last CNav solution as the current best state estimate for the next CNav solution. However, this leads to a overly conservative estimation of CNav's behavior, as this will mean that in a loss-of-solution event an at least 2 s old pose is used as the current best estimate. This will likely lead to tracking mode failing while in the real se-up with a navigation filter propagating the state in-between measurements tracking mode would still be able to track the solution. As a next step, we are now using a filter which estimates the full state of the lander on the basis of CNav measurements. This filter originates from our earlier work on the Chang'e 3 data set and is discussed in detail in [4]. It is a unscented Kalman filter (UKF), taking into account the non-linearity of the CNav measurements. The CNav measurements are used in a tightly coupled manner. It has to be understood that this filter derives IMU like measurements from consecutive CNav results. This is not necessarily representative of the quality of the state estimation performance of a real performance of a navigation system with an IMU and additional sensors. However, the goal of this set up is to demonstrate that CNav can successfully obtain, track and re-obtain the solution during a descent to the south pole flying over shaded regions.
Figure 7 shows the performance on the approximately last 700 s before touch down. It can be seen that the system can more or less continuously provide a CNav solution, there are short phase around 100 s and 300 s where the solution is lost for short periods of time. During these periods, the camera moves over large shaded areas where no craters can be detected anymore. However, even our simple filter set-up is able to track the state well enough that CNav can immediately pick up the solution again even after flying over these shaded areas.
Overall we were able to demonstrate that CNav can obtain successful valid solutions up to 600 m above the landing site.
Figure 8 presents the number of craters passed to the filter at every time instance. It can be seen that the number of matchable craters varies over the descent, up to 60. Here it should be noted, that in a real system it is not necessary to use all the matches inside the filter. Again the phases around 100 s and 300 s where no successful matches were made can be seen (indicated red).
Figure 9 presents six of the rendered images with the CNav results overlayed. It can be seen that the detector detects many craters(red circles) and successful matches are made(turquoise boxes). Moreover it can be seen that even with larger regions of shadow present in the images, successful solutions can be obtained.

5 CONCLUSION AND FURTHER WORK

We have been able to demonstrate that crater navigation can successful be used to land at the lunar south pole, even though the illumination conditions are challenging. Using the crater navigation in conjunction with a simple filter set-up we were able to achieve successful solutions up to 600 m above the landing site. We can therefore conclude that crater navigation is a viable means to observe a lander's absolute pose during south pole landing missions.

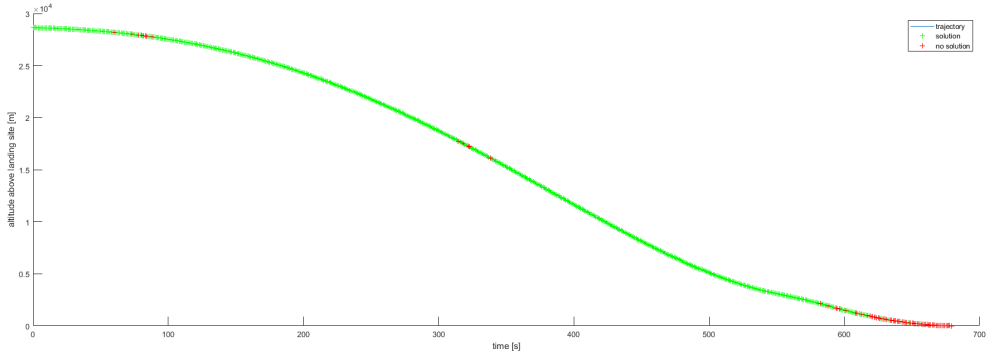

Figure 7: CNav Performance on Polar Descent Trajectory

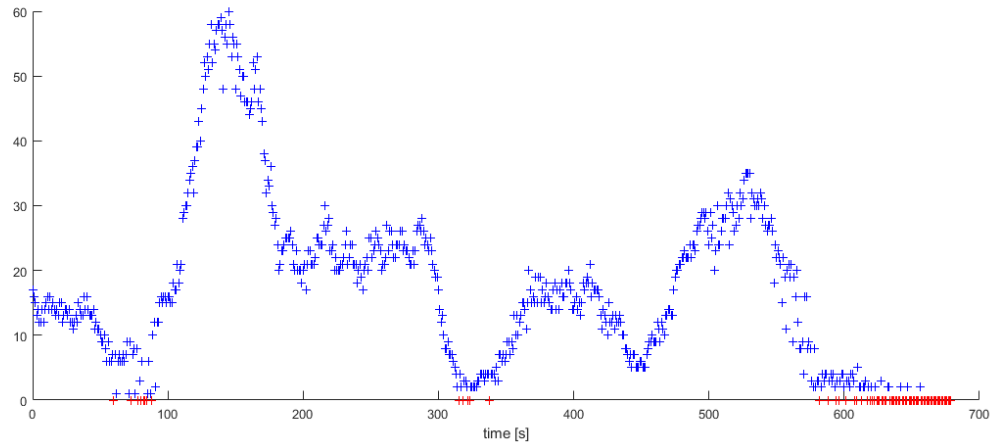

Figure 8: Number of craters passed to filter.

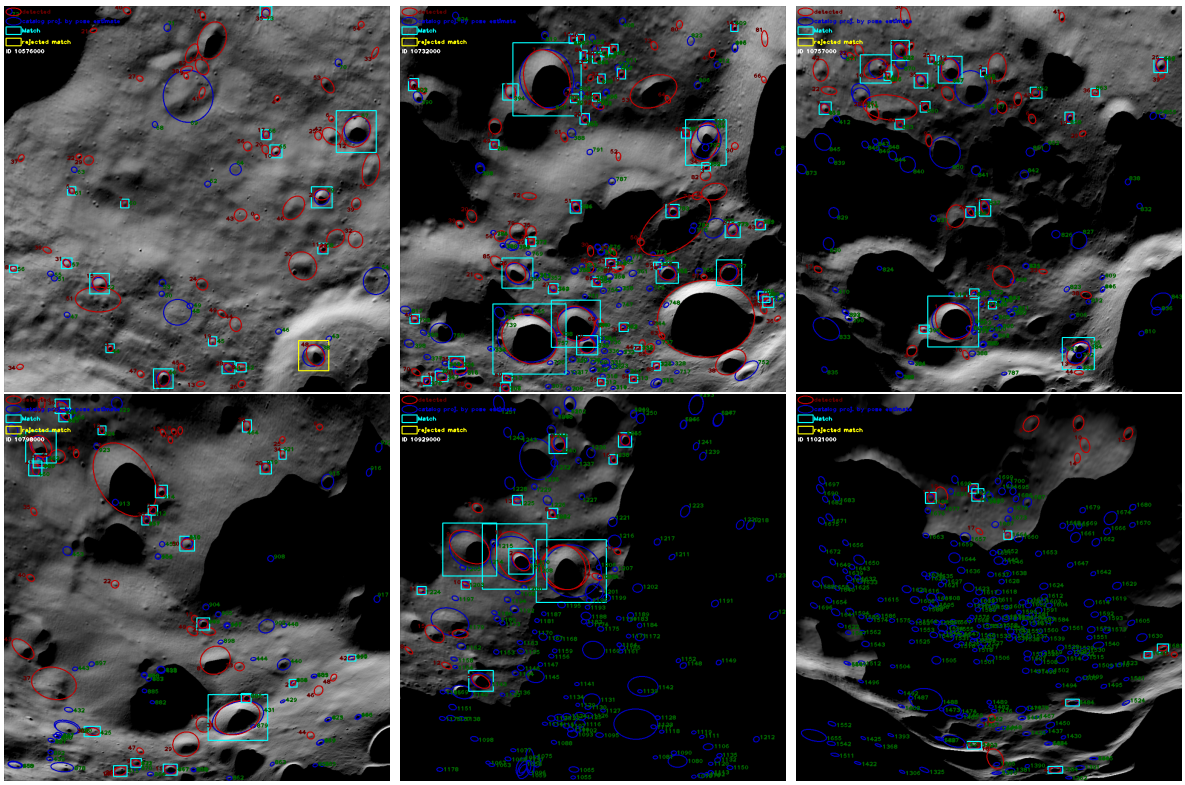

Figure 9: Some sample images with overlayed results.

Further work will go in several directions. One, within the EU project SENAV SENAVHomepage, is to explore options to store the global crater database onboard the spacecraft along with the missionization algorithms. Here robustness will be increased for back up maneuvers, and new applications will open up, such as continuous pose estimation for orbiters. Also, the current missionisation effort will be decreased. The same EU project will also look into acceleration of the CNav lost-in-space matching stage. Besides the software stage further hardware in the loop testing will be performed.

REFERENCES

[1] A. E. Johnson, S. B. Aaron, H. Ansari, C. Bergh, H. Bourdu, J. Butler, J. Chang, R. Cheng, Y. Cheng, K. Clark, et al., "Mars 2020 lander vision system flight performance," in AIAA SciTech 2022 Forum, 2022, p. 1214.

[2] B. Maass, "Robust approximation of image illumination direction in a segmentation-based crater detection algorithm for spacecraft navigation," CEAS Space Journal, vol. 8, no. 4, pp. 303–314, 2016. [Online]. Available: https://doi.org/10.1007/s12567-016-0129-1.

[3] B. Maass, H. Krüger, and S. Theil, "An edge-free, scale-, pose-and illumination-invariant approach to crater detection for spacecraft navigation," in 2011 7th International Symposium on Image and Signal Processing and Analysis (ISPA), IEEE, 2011, pp. 603–608.

[4] B. Maass, S. Woicke, W. M. Oliveira, B. Razgus, and H. Krüger, "Crater navigation system for autonomous precision landing on the moon," Journal of Guidance, Control, and Dynamics, vol. 43, no. 8, pp. 1414–1431, 2020.

[5] S. T. team, "Selene morning map," 2013, SELENE MOON TC 5 MORNING MAP V4.0, SELENE Data Archive. [Online]. Available: https://data.darts.isas.jaxa.jp/pub/pds3/sln-l-tc-5-morning-map-v4.0/.

[6] M. Barker, E. Mazarico, G. Neumann, M. Zuber, J. Haruyama, and D. Smith, "A new lunar digital elevation model from the lunar orbiter laser altimeter and selene terrain camera," Icarus, vol. 273, pp. 346–355, 2016, ISSN: 0019-1035. DOI: https://doi.org/10.1016/j.icarus.2015.07.039. [Online]. Available: https://www.sciencedirect.com/science/article/pii/S0019103515003450.

[7] G. Neumann, "2009 lunar orbiter laser altimeter raw data set, lro-l-lola-4-gdr-v1.0, nasa planetary data system," 2010, LDEM_60S_60M. DOI: https://doi.org/10.17189/1520642. [Online]. Available: https://ode.rsl.wustl.edu/moon/indexproductpage.aspx?product_idgeo=21746095&product_id=LDEM_60S_60M.LBL.

[8] D. De Rosa, B. Bussey, J. T. Cahill, T. Lutz, I. A. Crawford, T. Hackwill, S. van Gasselt, G. Neukum, L. Witte, A. McGovern, P. M. Grindrod, and J. D. Carpenter, "Characterisation of potential landing sites for the european space agency's lunar lander project," Planetary and Space Science, vol. 74, no. 1, pp. 224–246, 2012, Scientific Preparations For Lunar Exploration, ISSN: 0032-0633. DOI: https://doi.org/10.1016/j.pss.2012.08.002. [Online]. Available: https://www.sciencedirect.com/science/article/pii/S0032063312002395.

[9] C. Acton, N. Bachman, B. Semenov, and E. Wright, "A look towards the future in the handling of space science mission geometry," Planetary and Space Science, vol. 150, pp. 9–12, 2018, Enabling Open and Interoperable Access to Planetary Science and Heliophysics Databases and Tools, ISSN: 0032-0633. DOI: https://doi.org/10.1016/j.pss.2017.02.013. [Online]. Available: https://www.sciencedirect.com/science/article/pii/S0032063316303129.

[10] G. Neumann, "2009 lunar orbiter laser altimeter raw data set, lro-l-lola-4-gdr-v1.0, nasa planetary data system," 2010, LDEM_875S_20M. DOI: https://doi.org/10.17189/1520642. [Online]. Available: https://ode.rsl.wustl.edu/moon/indexproductpage.aspx?product_idgeo=21746145&product_id=LDEM_875S_20M.

[11] C. Paproth, E. Schlüßler, P. Scherbaum, and A. Börner, "Sensor++: Simulation of remote sensing systems from visible to thermal infrared," in XXIInd ISPRS Congress, ser. ASPRS, vol. XXXIX, ISPRS, Sep. 2012, pp. 257–260. [Online]. Available: https://elib.dlr.de/77229/.